International Journal of Smart Home
Vol. 10, No. 9 (2016), pp. 93-102
http://dx.doi.org/10.14257/ijsh.2016.10.9.09

Segmentation of the Synthetic Aperture Radar Image Using the Watershed Transformation and Region Merging Technique

Chuanxian Jiang[1], Zhiping Li[2*], Xiaohui Chen[1], Zejun Zhang[3], Yeqing Yi[4]

[1]*School of Information Science and Engineering, Guilin University of Technology, Guilin 541004, China*
[2]*Department of Science, Hainan College of Software Technology, Qionghai 571400, China*
[3]*School of Computer and Information Science, Fujian Agriculture and Forestry University, Fuzhou 35002, China*
[4]*Department of Information Science and Engineering, Hunan University of Humanities Science and Technology, Loudi 417000, China*
emlong1976@tom.com

Abstract

This paper presents an efficient algorithm that segments the synthetic aperture radar (SAR) image into several homogeneous regions by combining edge- and region-based information. A multi-direction ratio edge detector is used to capture the locally directional variation information of a SAR image and construct the ratio edge strength map (RESM) of the SAR image. Watershed transformation is performed on the thresholded RESM to obtain an over-segmentation result. An efficient hierarchical region merging procedure based on the region adjacency graph representation of the image regions is proposed. A novel dissimilarity measurement between the two adjacent regions is derived from the multiplicative noise speckle model of the multi-look SAR image. Experimental results and the performance evaluation show that the proposed method outperforms two widely used SAR image segmentation approaches.

Keywords: *Synthetic aperture radar (SAR), Image segmentation, Watershed transformation, Region adjacency graph (RAG)*

1. Introduction

In recent decades, synthetic aperture radar (SAR) imaging systems have been widely used in many applications, such as remote sensing [1,2]. These systems offer a high image solution at any time of the day in all weather conditions. However, the speckle noise of the imaging system [3] renders the images grainy and severely deteriorates the performance of SAR image automatic interpretation. SAR image segmentation [4,5] is crucial to low levels of SAR image automatic interpretation; such segmentation provides information on the structures in an image by partitioning the image into a number of homogeneous regions. To reduce the speckle noise in SAR image segmentation, a large effort has been made using some statistical properties of the image.

[1]Edge-based SAR image segmentation methods have been proposed to identify the transitions between homogeneous areas using a ratio edge detector [6]. Within this community, thresholding and morphological operations are applied to obtain single-pixel-wide and closed contours. However, this technique is still far from obtaining satisfactory segmentation results.

Zhiping Li is the corresponding author.

ISSN: 1975-4094 IJSH

Region-based SAR image segmentation methods identify directly the regions using the predefined homogeneity criteria. These methods first partition a given image into a set of homogeneous over-segmented regions and then merge the similar adjacent regions to create new large regions [7,8]. Region growing [9,10] and region split-and-merge techniques [11–13] are widely used to over-segment an image into homogeneous primitive regions. The former is a bottom-up method that iteratively merges pixels into sets growing from the initial selected seed set [9]. The segmentation results produced by the region growing method have an inherent dependency on the selection of initial seed points [14] and the design of regional growing criteria [7]. On the contrary, the region split-and-merge approach first partitions a given image into initial homogeneous regions using a top-down strategy, which iteratively divides a rectangular region into four sub-rectangular regions until no heterogeneous region is evident within the image. A region merging procedure is then adopted to fuse the similar adjacent regions. The boundaries of the regions in the image achieved by this method are composed of long horizontal and vertical segments. The split-and-merge approach is also sensitive to the definition of the region homogeneity test [11,12].

To obtain improved segmentation results, many combination methods integrating edge and region information have been proposed [15]. A unifying framework of these methods consists of two stages. The first stage involves over-segmentation, in which a simple and efficient initial partition method is used to obtain the over-segmentation results of a SAR image. The second stage involves region merging, which iteratively merges the most similar two adjacent regions in the initial over-segmentation results until a predefined terminate condition is met. The core of the region merging technique is the design of dissimilarity measures between two adjacent regions. Some dissimilarity measures are deduced from minimizing an energy (objective) function [16], whereas others are based on the moments estimated from the image data [17]. In the present study, a dissimilarity measurement of two adjacent regions is induced from the multiplicative noise model of a multi-look SAR image.

An efficient SAR image segmentation algorithm is proposed in this study. Watershed transformation [18] and ratio edge detector are used to obtain the over-segmentation results of a SAR image. The region merging technique is also utilized with a novel region merging criterion to produce final segmentation results. A novel region merging criterion is proposed based on the proposed new dissimilarity measurement induced from the multiplicative noise model of multi-look SAR image and a boundary-length penalty term. Segmentation results are represented by the region adjacency graph (RAG), [15] which is an undirected graph, whose nodes identify regions of the segmentation results and edges determine neighborly relations between regions.

The rest of this paper is organized as follows. Section 2 describes the image segmentation problem and then proposes the skeleton of the segmentation algorithm. Section 3 discusses the initial partition results obtained using a multi-directional ratio edge detector and watershed transformation. Section 4 focuses on the design of the dissimilarity measurement of a pair of adjacent regions and the bottom-up hierarchical region merging method. Section 5 presents the segmentation results on synthetic and real SAR images and reports a performance evaluation of the proposed segmentation algorithm. Finally, Section 6 ends with the conclusion.

2. Problem Formulation and Algorithm Skeleton

Assume that an image I consists of $N = N_x \times N_y$ pixels: $I = \{I(x,y) \mid (x,y) \in S\}$, $S = \{(x,y) \mid 1 \le x \le N_x, 1 \le y \le N_y\}$ denotes the discrete rectangular lattice and tessellated of R statistically independent and homogeneous regions $\Re^R = \{\Omega_r, r = 1, 2, \cdots, R\}$, and each region contains N_r pixels. The region Ω_r is limited by a closed contour $\partial\Omega_r$. The tessellated region $\Re^R = \{\Omega_r, r = 1, 2, \cdots, R\}$ and their closed contour $\partial\Re^R = \{\partial\Omega_r, r = 1, 2, \cdots, R\}$ form a segmentation of the SAR image as follows:

1) $\forall i \neq j, \Omega_i \cap \Omega_j = \varnothing$

2) $\left(\cup_{i=1}^{R}\Omega_i\right) \cup \left(\cup_{i=1}^{R}\partial\Omega_i\right) = S$

3) $\forall i \neq j, \partial\Omega_i \cap \partial\Omega_j \neq \varnothing \Leftrightarrow$ Regions Ω_i and Ω_j are adjacent.

The skeleton of the proposed segmentation algorithm mainly consists of two stages: initial partition based on a multi-direction ratio edge detector and watershed transformation and iterative region merging process with the proposed novel region merging criterion.

In the first stage of this algorithm, a multi-directional ratio edge detector is used to construct the ratio edge strength map (RESM) of an image. The watershed transformation on the thresholded RESM is subsequently applied to obtain an initial partition of the SAR image. The obtained initial partition is represented by $\Re^R$. In the second stage, an iterative bottom-up hierarchical region merging approach is used to integrate the most similar pair of adjacent regions until a predefined stopping criterion is met.

3. Initial Partition

In this section, a multi-direction ratio edge detector [19] is applied to construct the RESM of a SAR image. Figure 1 shows the graphic representation of the edge detector with a specific angle, which is described by a parameter configuration $K_f = \{l_f, w_f, d_f, \theta_f\}$, the length, the width, the spacing of the filter, and the angle θ_f between two orientations. A detector with angle θ_f first estimates the means on each side of the central pixel (x, y), $\hat{R}_1(x, y, \theta)$ and $\hat{R}_2(x, y, \theta)$. One can then obtain a ratio of the two means along the orientation:

$$r(x, y, \theta) = \min\left(\frac{\hat{R}_1(x, y, \theta)}{\hat{R}_2(x, y, \theta)}, \frac{\hat{R}_2(x, y, \theta)}{\hat{R}_1(x, y, \theta)}\right). \tag{1}$$

The ratio edge detector with different orientations is scanned in the image in succession and, for each pixel (x, y), taking the minimum response over orientations yields $RESM(x, y)$,

$$RESM(x, y) = 1 - \min_{\theta}\{r(x, y, \theta)\}. \tag{2}$$

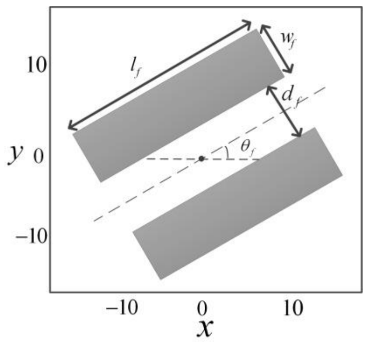

Figure 1. Multi-Direction Ratio Edge Detector

The morphological watershed transformation of the RESM is an excellent method to extract an initial partition of a SAR image [22]. This method can be used to partition an image into several regions that are delimited by continuous and one-pixel-wide closed contours. The number of the partitioned regions is determined by one of the regional minima in the RESM. From a practical point of view, most of the regional minima in the RESM are caused by the noise in the image, and pre-processing must be conducted to suppress these regional minima prior to the watershed transform.

The preprocessing of RESM aims to alleviate over-segmentation in homogeneous regions, which is produced by the regional minima in the RESM. The strength of the RESM in the homogeneous regions is lower than that along the boundaries between two adjacent regions. Hence, the regional minima can be suppressed using a simple threshold operator. Specifically, the regional minima are replaced by fewer zero-valued regional minima in the thresholded RESM. The thresholded RESM is

$$RESM_T\left(x,y\right)=\begin{cases} RESM\left(x,y\right), & if\ RESM\left(x,y\right)>T \\ 0, & otherwise \end{cases} \quad . \tag{3}$$

The determination of the threshold value T is directly based on the global histogram estimation of the RESM

$$T=hist\left(n\right) \quad with \quad n=\arg\min_{m}\left\{m \mid \alpha \le \sum_{i=1}^{m} hist\left(i\right)\right\} \tag{4}$$

where $hist\left(i\right)$ and α are the global histogram of the RESM and its percentile, respectively.

An over-segmentation result is obtained by the watershed transformation [20] of the thresholded RESM $RESM_T\ (x, y)$.

4. Hierarchical Region Merging

4.1. Dissimilarity Measurement

The dissimilarity measurement between a pair of adjacent regions is deduced from the moments of the probability-density function of the SAR amplitude derived from an n-look multiplicative noise model. Let Ω_1 , $\Omega_2 \in \Re^R$ be a pair of adjacent regions. The dissimilarity measurement between these two regions can be defined as follows:

$$\upsilon\left(\Omega_1,\Omega_2\right)=\left(1-\min\left(\frac{X_1}{X_2},\frac{X_2}{X_1}\right)\right)\Bigg/\sqrt{\frac{1}{2}\cdot\left(\alpha+\beta\right)\cdot\left(\frac{1}{N_1}+\frac{1}{N_2}\right)} \tag{5}$$

where $N_i, i=1,2$ is the number of pixels in regions Ω_1 and Ω_2, respectively. $X_i=\frac{1}{N_i}\sum_{(x,y)\in\Omega_i} I\left(x,y\right),\ i=1,2$, $\alpha=\frac{\left(4-\pi\right)}{\pi L}$, $\beta=\frac{\left(6-2\pi\right)}{\pi L}$, and L is the number of looks of the SAR image.

Image segmentation is an inverse problem and is generally ill posed from a mathematical point of view; hence, the regularization method [21] is introduced to obtain meaningful segmentation results. In this paper, a penalty term, which is defined as the length of the common boundary between these two adjacent regions, is added to the dissimilarity measurement $\upsilon\left(\Omega_1,\Omega_2\right)$ to construct the proposed region merging criterion:

$$\kappa\left(\Omega_1,\Omega_2\right)=\upsilon\left(\Omega_1,\Omega_2\right)+\lambda\cdot\left(\left|\partial\Omega_1\cap\partial\Omega_2\right|\right)^{-1} \tag{6}$$

where λ is a tradeoff factor between the dissimilarity measurement and common boundary length penalty term, which is determined previously and heuristically. $|A|$ is the cardinality of the argument A.

The final segmentation result is obtained by iteratively merging the most similar adjacent region pair in the initial over-segmentation using the region merging algorithm with the region merging criterion (6). Once a pair of adjacent regions whose merging criterion is lower than a certain threshold is found, the merging process is terminated.

4.2. Iterative Region Merging

The RAG is used to represent the partition results. The RAG of a *R*-partition $\Re^R$ is defined as an undirected graph, $G=(V,E)$, where $V=\{1,2,\cdots,R\}$ is a set of nodes and $E\subset V\times V$ is the set of edges. In the segmentation results, each region is represented by a graph node and an edge $(i,j)\in E$ if regions i and j are adjacent. Each edge in E is assigned a weight that denotes the merging criterion between the two adjacent regions, and the edge with the minimum weight corresponds to the most similar pair of adjacent regions. In each iterative region merging procedure, the edge with the minimum weight is removed from RAG G, while G is updated simultaneously. This recursive algorithm does not stop until the minimum weight is greater than a certain threshold.

Algorithm 1 is described in Figure 2, which directly uses RAG to implement the region merging procedure. The input of **algorithm 1** is the initial over-segmentation results of a given image, which results from the watershed transformation of the preprocessed RESM. Based on the over-segmentation, a RAG is established as the data construction of a region merging algorithm. In each iteration of the merging algorithm, a scan of all the edges in set *E* is required to determine the edge with the minimum weight. From the algorithmic point of view, the search can be implemented using the bottom-up heap construction method in $O(\|E\|)$ time. During the period of region merging, all the edges of the RAG are stored in the heap. The edge with the minimum weight is removed from the heap in $O(\log_2(\|E\|))$ time (*i.e.*, moving the remaining items in the heap to satisfy a certain relationship with other items), and the corresponding nodes connected by the edge are merged, which updates both the RAG and the heap. Specifically, the minimum edge and its related two nodes are removed from the RAG. A new node is produced, merging the two adjacent regions represented by the two nodes. The new node is added to the RAG and linked with the nodes connected with one of the two removed nodes. Simultaneously, the weights of these new edges are updated by recalculating their region merging criterion, requiring $O(\|E\|)$ time to search an item that needs to be updated in the heap and $O(\log_2(\|E\|))$ time for updating it. Thus, in each iteration, $O(d\cdot\|E\|\cdot\log_2(\|E\|))$ time is needed to update all the edges involved with the new node produced by removing the edge with the minimum weight, where *d* denotes the degree of this new node.

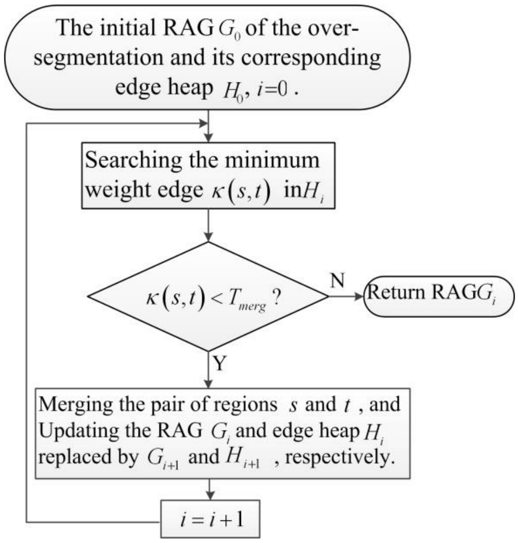

Figure 2. Algorithm 1. Region Merging Process using RAG

5. Experiments and Performance Evaluation

5.1. Experiments for Synthetic and Real SAR Images

In this subsection, we illustrate the experimental results of synthetic and real SAR images using the proposed segmentation algorithm.

In all of our experiments, the value of percentile α in the threshold processing of RESM is equal to 0.3. The parameter λ in (6) is equal to 30 for all of our experiments. The predefined region merging threshold T_{merg} is 50.

In addition, we compare the results produced by the proposed segmentation algorithm with those produced by two widely used SAR image segmentation algorithms. One of the methods is the SRG, which is based on statistical region growing and hierarchical merging [17], and the other is the CHUMSIS, which uses a context-based hierarchical unequal region merging approach to segment a SAR image into several homogeneous regions [22].

Synthetic images: To verify the proposed segmentation approach, we first present our segmentation results on synthetic cartoon images with speckle noise. We simulate one-, three-, and five-look amplitude synthetic images. Each image is composed of 512×479 pixels, comprising 37 regions, and their contrasts of the means of adjoining regions vary from 1.2 to 8.5 (see Figure 3).

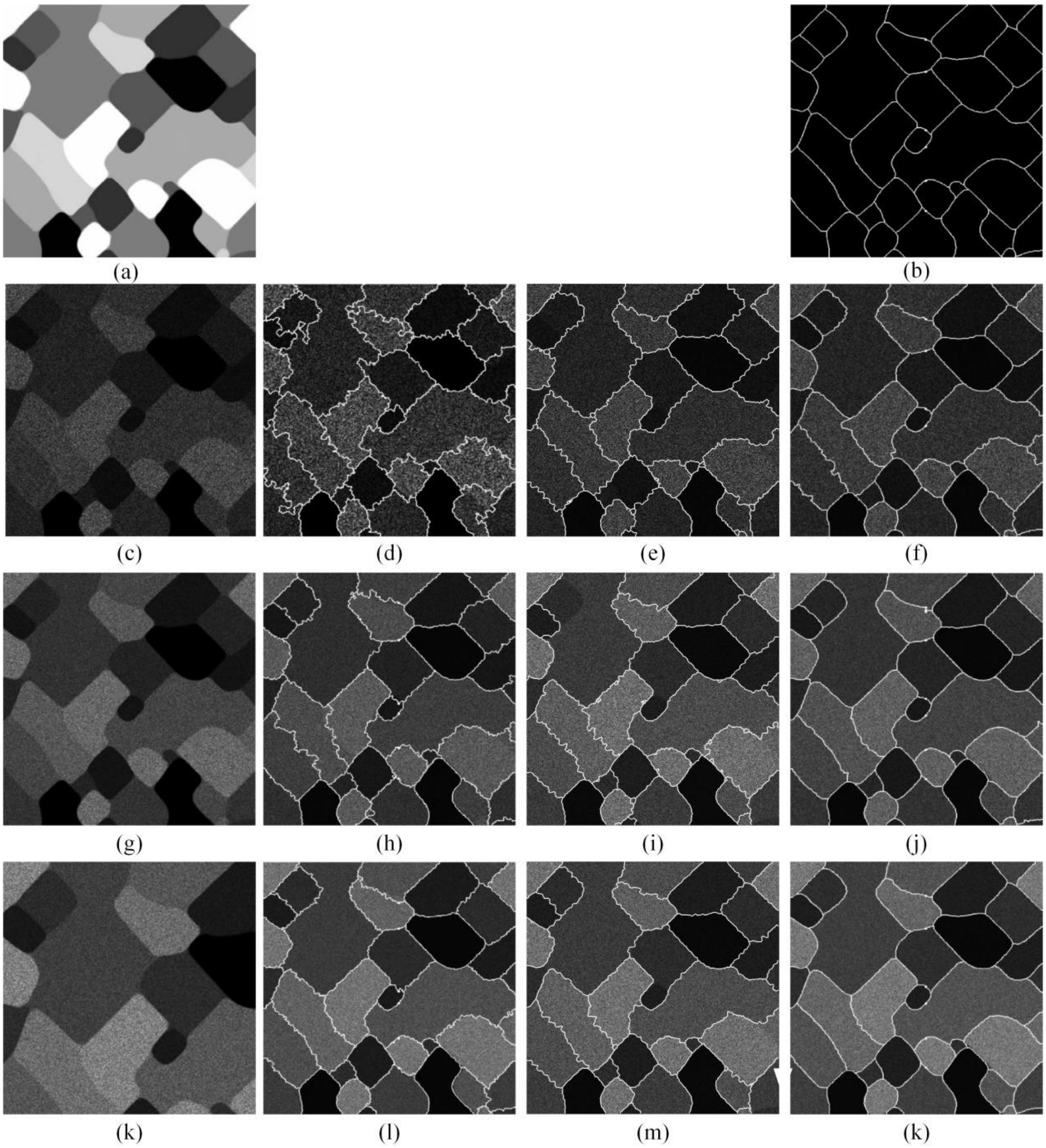

Figure 3. Segmentation of Synthetic Images. (a) Synthetic Cartoon Image [18] (512×479) composed of 37 Regions with Different Contrasts Varying from 1.2 to 8.5; (b) ground truth of (a); (c), (g), and (k) are Simulated One-, Three-, and Five-look Amplitude SAR Images, Respectively; (d), (h) and (l) are the Final Segmentation Results using the SRG; (e), (i), and (m) are the Final Segmentation Results Produced by the CHUMSIS; (f), (j), and (k) Are the Final Segmentation Results Produced by the Proposed Algorithm

Real SAR images: Now, we test the proposed method on real SAR images (see Figure 4).

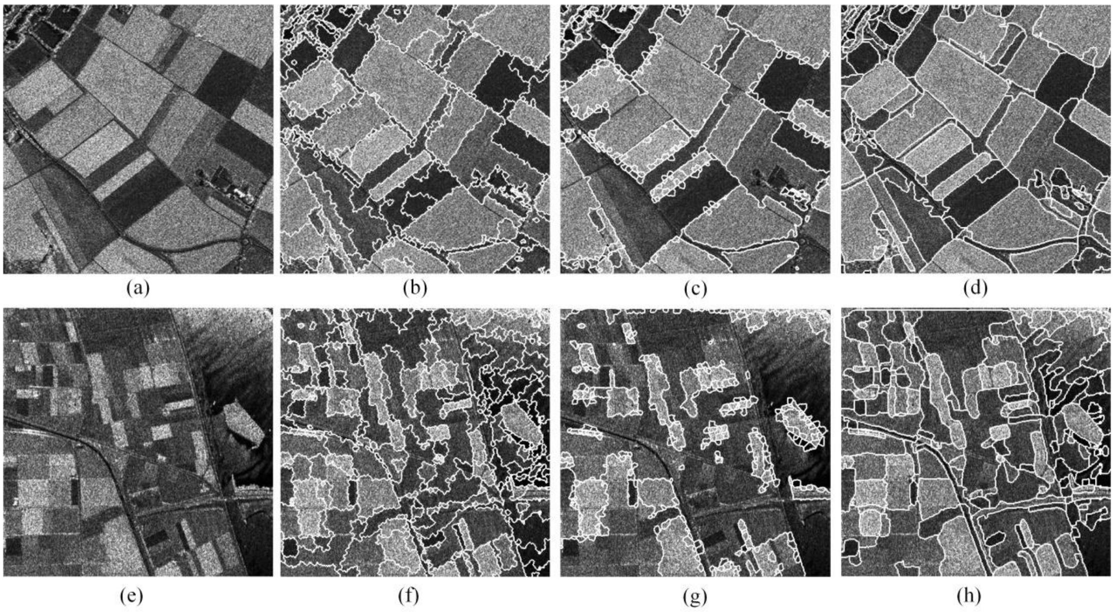

Figure 4. Extract of a Three-Look Amplitude SAR Image. (a) 400×401 Pixels and (e) 400×401 Pixels are Two Real SAR Images; (b) and (f) are the Final Segmentation Results using the SRG; (c) and (g) are the Final Segmentation Results using the CHUMSIS; (d) and (h) are the Final Segmentation Results produced by the Proposed Algorithm

5.2. Performance Evaluation

We compare the proposed segmentation algorithm with the SRG and the CHUMSIS by applying a set of simulated test images derived from a single synthetic cartoon image (see Figure 3(a)). The “ground truth” of the synthetic image is identified and is used to evaluate the performance of different segmentation results produced by different algorithms. To test the performance of the proposed method on a multi-look SAR image, we develop three sets of test images based on one-, three-, and five-look. Each set consists of 30 independently populated images. Figures 3(c), (g), and (k) illustrate a representation of the one-, three-, and five-look data sets, respectively.

We evaluate the performance of the proposed method using the boundary quality measure based on the boundary-based precision-recall framework [23]. The edge localization performance of the proposed segmentation method can be evaluated by the precision-recall framework [23] based on the set of simulated test images with the ground truth. Given the detected edge map E and its corresponding ground truth GT, which are both binary images with 1’s indicating edge pixels, we can calculate the precision (P) and recall (R) as follows:

$$P = \sum_{\boldsymbol{x}} \boldsymbol{GT}(\boldsymbol{x}) \cdot E(\boldsymbol{x}) \Big/ \sum_{\boldsymbol{x}} E(\boldsymbol{x}), \quad R = \sum_{\boldsymbol{x}} \boldsymbol{GT}(\boldsymbol{x}) \cdot E(\boldsymbol{x}) \Big/ \sum_{\boldsymbol{x}} \boldsymbol{GT}(\boldsymbol{x}), \tag{7}$$

where $\boldsymbol{x} = (x_1, x_2)$ is a vector that represents a coordinate on the image plane. The precision P is the probability that the detected edge pixels are valid, and the recall R is the probability that the ground truth edge pixels are detected (*i.e.*, hit rate). The overall performance measurement F-measure (F) is the weighted harmonic mean of precision and recall with a non-negative β:

$$F = PR \big/ \left(\beta R + (1-\beta) P\right), \tag{8}$$

where we set $\beta = 0.5$, following [23].

Table 1 shows the precision, recall, and F-measure of different segmentation algorithms on these three data sets. The ideal value of the precision and recall is 1. Thus, larger values of the precision and recall indicate a better performance of the segmentation algorithm. In our experiments, the recommended parameters of SRG and CHUMSIS are used to obtain satisfying segmentation results. Table 1 reveals that the proposed method outperforms SRG and CHUMSIS.

Table 1. Comparison of the Methods in Terms of Recall, Precision, and F-Measure when Selecting an Optimal Threshold for the Three Data Sets

Original image	SRG			CHUMSIS			Proposed method		
	R	*P*	*F*	*R*	*P*	*F*	*R*	*P*	*F*
One-Look	0.79	0.61	0.69	0.64	0.77	0.70	0.95	0.92	0.93
Three-Look	0.89	0.75	0.81	0.75	0.84	0.79	0.98	0.95	0.96
Five-Look	0.92	0.80	0.86	0.78	0.87	0.82	0.98	0.96	0.97

6. Conclusion

A SAR image segmentation approach using edge- and region-based information is proposed in this study. The initial over-segmentation is obtained from the watershed transformation of the thresholded RESM extracted by the multi-direction ratio edge detector. A dissimilarity measurement is designed between neighboring regions based on a multi-look multiplicative noise model. Considering computational efficiency, we develop a method that can be quickly implemented using the RAG. The experiments conducted on the synthetic and real SAR images indicate the efficiency of the proposed algorithm compared with two widely used SAR image segmentation algorithms.

In our future work, we will generalize the model to consider the multiplicative speckle in SAR images and the nonstationary property of such images to enhance the segmentation performance further.

Acknowledgements

This work was supported by the National Natural Science Foundation of China (Grant Nos. 61262076,61262075,61472135), the Natural Science Foundation of Hainan Province, China（Grant No. 20161008）,and the Natural Science Foundation of Guangxi Province, China(Grant No. 2014GXNSFAA118379).

References

[1] T. L. Toan, F. Ribbes, L. F. Wang, N.Floury,K.H.Ding. Rice crop mapping and monitoring using ERS-1 data based on experiment and modeling results. IEEE Trans. Geosci. Remote Sensing, Vol.35, No.1,**(1997)**,pp. 41-56.

[2] H. Yu, L.C. Jiao, F. Liu. Context based unsupervised hierarchical iterative algorithm for SAR segmentation. Acta Automatica Sinica, Vol.40, No.1,**(2014)**,pp.100-116(in Chinese）.

[3] J. W. Goodman. Statistical properties of laser speckle patterns. Laser Speckle and Related Phenomena Topics in Applied Physics, Vol. No.9,**(1975)**,pp.9-75.

[4] P.Zhang, M.Li, Y.Wu, and H.Li .Hierarchical Conditional Random Fields Model for Semisupervised SAR Image Segmentation. IEEE Trans. Geosci. Remote Sensing, Vol. 53, No. 9, **(2015)**,pp.4933-4951.

[5] D.Xiang, T.Tang, C.Hu, Y.Li, and Y.Su. A Kernel Clustering Algorithm With Fuzzy Factor:Application to SAR Image Segmentation. IEEE Geoscience and Remote Sensing Letters, Vol.11, No. 7, **(2014)**,pp.1290-1294

[6] O. Germain and P. Regregier. On the bias of the likelihood ratio edge detector for SAR images. IEEE Trans. Geosci. Remote Sensing, Vol.38, No.3,**(2000)** ,pp.1455-1458.

[7] B. Peng, L. Zhang and D. Zhang. Automatic image segmentation by dynamic region merging. IEEE Trans. Image Processing, Vol.12, No.12,**(2011)** ,pp.3592-3605.
[8] Q. Yu and D. A. Clausi. IRGS: Image segmentation using edge penalties and region growing. IEEE Trans. Pattern Anal. Mach. Intell. , Vol.30, No.12,**(2008)** ,pp.2126-2139.
[9] S. A. Hojjatoleslami and J. Kittler. Region growing: A new approach. IEEE Trans. Image Processing, Vol.7, No.7,**(1998)**,pp.1079-1084.
[10] S. Y. Wan and W. E. Higgins. Symmetric region growing. IEEE Trans. Image Processing, Vol.12, No.9,**(2003)** ,pp.1007-1015.
[11] R. Nock and F. Nielsen. Statistical region merging. IEEE Trans. Pattern Anal. Mach. Intell. , Vol.26, No.11,**(2004)** ,pp.1452-1458.
[12] X. Wu. Adaptive split-and-merge segmentation based on piecewise least-square approximation. IEEE Trans. Pattern Anal. Mach. Intell., Vol.15, No.8,**(1993)** ,pp.808-815.
[13] B.Anton,R.Jaume,B.Imma,F.Miquel,S.Mateu. Image segmentation using information bottleneck method. IEEE Trans. Image Processing, Vol.18, No.7,**(2009)** ,pp.1601-1612.
[14] R. Adams and L. Bischof. Seeded region growing. IEEE Trans. Pattern Anal. Mach. Intell., Vol.16, No.6,**(1994)** ,pp.641-647.
[15] K. Haris, S. N. Efstratiadis, N. Maglavers and A. K. Katsaggelos. Hybrid image segmentation using watersheds and fast region merging. IEEE Trans. Image Processing, Vol.7, No.12,**(1998)** ,pp.1684-1699.
[16] Q. Luo and T. M. Khoshgoftaar. Unsupervised multiscale color image segmentation based on MDL principle. IEEE Trans. Image Processing, Vol.15, No.9,**(2006)** ,pp.2755-2761.
[17] E. A. Carvalho, D. M. Ushizima, F. N. S. Medeiros, C. I. O. Martins, R. C. P. Marques. SAR imagery segmentation by statistical region growing and hierarchical merging. Digital Signal Processing, Digital Signal Processing, Vol.20, No.5,**(2009)** ,pp.1365-1378.
[18] L. Vincent and P. Soille. Watersheds in digital spaces: An efficient algorithm based on immersion simulations. IEEE Trans. Pattern Anal. Mach. Intell., Vol. 13, No.6,**(1991)**,pp.583-598.
[19] J. Schou, H. Skriver, A. A. Nielsen and K. Conradsen. CFAR edge detector for polarimetric SAR images. IEEE Trans. Geosci. Remote Sensing, Vol. 41, No.1,**(2003)**,pp.20-32.
[20] W. Li, G. B. Benie, D. C. He,S. Wang,D.Ziou. Watershed-based hierarchical SAR image segmentation. Int. J. Remote Sens., Vol.20, No.17,**(1999)** ,pp.3377-3390.
[21] T. Poggio, V. Torre and C. Koch. Computational vision and regularization theory," nature, Vol.317, No.26,**(1985)** ,pp.314-319.
[22] H. Yu, X. Zhang, S. Wang, B.Hou. Context-based hierarchical unequal merging for SAR image segmentation.IEEE Trans. Geosci. Remote Sensing, Vol.51, No.2,**(2013)** ,pp.20-32.
[23] D. R. Martin, C. C. Fowlkes, and J. Malik. Learning to detect natural image boundaries using local brightness, color and texture cues. IEEE Trans. Pattern Anal. Mach. Intell.,Vol.26, No.5,**(2004)** ,pp. 530-549.

